Neutron radiography study of hydrogen desorption in technical iron

K. Beyer · T. Kannengiesser · A. Griesche · B. Schillinger

Abstract The purpose of the present study is to show the feasibility of examining hydrogen desorption in technical iron samples using neutron radiography at the ANTARES facility of the FRM II research reactor, Technische Universität München. It has been shown that this method is appropriate for in situ determination of hydrogen desorption for concentrations as low as 20 ppm_H. Experiments were carried out in the temperature range from room temperature up to 260 °C. Measurement was based on direct comparison between electrochemically hydrogen-loaded iron samples and hydrogen-free reference samples at the same temperature. This enables the determination of hydrogen concentration as a function of time and temperature. Ex situ carrier gas hot extraction experiments using the same temperature–time profiles as the neutron radiography experiments have been used to calibrate the greyscale values of the radiographs to defined hydrogen concentrations. It can be stated that hydrogen desorption correlates with sample temperature.

Introduction

The study of metal–hydrogen systems has been a topic of considerable scientific research for many years. Hydrogen can limit the durability of iron and iron-based alloys due to degradation of mechanical properties and hydrogen-assisted cracking. The hydrogen transport processes in steels have been widely discussed in several reviews [1–5]. In general, hydrogen uptake can occur during welding, causing hydrogen-assisted cold cracking, as well as during service, causing hydrogen-assisted stress corrosion cracking. Various models have been postulated to describe the complex mechanisms leading to hydrogen-assisted cracking [6–10]. The two most widely accepted mechanisms are 'hydrogen-enhanced localised plasticity' and 'hydrogen-enhanced decohesion' [11–13]. However, various questions remain concerning hydrogen mass transport in iron and iron-based alloys, particularly with regard to the diffusion mechanism and the accuracy of diffusion coefficients available in the literature. To track the evolution of the hydrogen distribution and to determine the hydrogen diffusion mechanism, it is necessary to measure the concentration of hydrogen locally. This facilitates investigation of hydrogen mass flow in complex microstructures and improves understanding of the role of microstructural features, e.g. grain boundaries, phase boundaries and precipitates, in hydrogen diffusion. Technical iron was chosen as a material of interest for studying the feasibility of neutron radiography as a method for in situ determination of hydrogen concentrations and diffusion coefficients, because it has the advantage of lacking microstructural effects such as precipitations, solid solutions, second phases or phase transformations in the investigated temperature range (phase transformation α-Fe to δ-Fe at 900 °C). Hydrogen has higher mobility in ferritic steels than in austenitic stainless steels due to the body-centred cubic structure of the lattice, which results in hydrogen embrittlement and blistering. This high mobility is reflected by a lower diffusion activation energy $E_A = 0.16$–0.18 eV [14] in ferritic steels than in Cr–Ni steels with $E_A = 0.52$–0.57 eV [15]. The high hydrogen mobility explains the low resistance of iron to hydrogen-assisted cracking.

K. Beyer (✉) · T. Kannengiesser · A. Griesche
BAM Federal Institute for Materials Research and Testing,
Unter den Eichen 87, 12205 Berlin, Germany
e-mail: katrin.beyer@bam.de

B. Schillinger
Technische Universität München, FRM II, 85748 Garching,
Germany

In general, in situ determination of small amounts of hydrogen in steels is difficult without destroying the sample. Typical methods, e.g. carrier gas hot extraction (CGHE) [16], transmission electron microscopy (TEM) and atomic force microscopy (AFM) [17–20], detect hydrogen indirectly or ex situ, or require complex sample preparation. A suitable method to avoid these disadvantages is neutron radiography (NR). NR has relatively high temporal resolution (~ 28 s per frame, including camera readout time) compared with the kinetics of hydrogen diffusion and suitable spatial resolution (~ 100 μm) compared with the characteristic diffusion length, and delivers visual information of the hydrogen concentration distribution. Another method is X-ray diffraction, which allows indirect observation of hydrogen by measuring lattice parameter expansion [21]. Neutron radiography is a nondestructive imaging method with a wide field of application in materials science, physics, biology and archaeology [22–26]. Neutrons interact directly with atomic nuclei, leading to both absorption and scattering of the neutrons. A neutron-sensitive detector records the transmitted neutrons, producing a two-dimensional (2D) attenuation distribution image. In general, the attenuation behaviour of matter is described by the Lambert–Beer law (Eq. 1)

$$I = I_0 \exp(-\mu d), \tag{1}$$

with measured intensity I, initial intensity I_0, linear attenuation coefficient μ, and total thickness of the sample d.

Experimental section

Materials and sample preparation

Technical iron samples with average grain size of 80 μm were used. The chemical composition is given in Table 1.

The samples were produced by cutting a rolled plate, with subsequent grinding and polishing of the surface to final surface roughness of 1 μm. The sample dimensions were 40 mm × 5 mm × 2 mm. Before loading with hydrogen, all samples were cleaned for 5 min with ethanol in an ultrasonic bath to remove mechanical and chemical residues.

Electrochemical hydrogen loading was carried out in a galvanostatically connected charging cell. As electrolyte, a solution consisting of 0.05 M H_2SO_4 and 0.1 M $NaAsO_2$ (ratio 1:500) was used. Sodium arsenide serves as a promoter to inhibit hydrogen recombination at the sample surface. A current density of 100 μA/mm^2 was applied for 48 h to fully saturate the cathodically connected sample with hydrogen. All samples were stored in liquid nitrogen to avoid hydrogen desorption after loading.

Sample characterisation

CGHE was applied to measure the amount of hydrogen loaded into the sample. In this method, hydrogen is activated by a heat treatment to diffuse to the surface, where it recombines and desorbs as H_2 into a constant flow of nitrogen. A calibrated sensor measures the change in the thermal conductivity of the N_2/H_2 gas mixture, which is a function of gas composition. Figure 1 shows a typical result of such an experiment. The extraction of hydrogen was performed under isothermal conditions at three different temperatures: 400 °C, 650 °C and 900 °C.
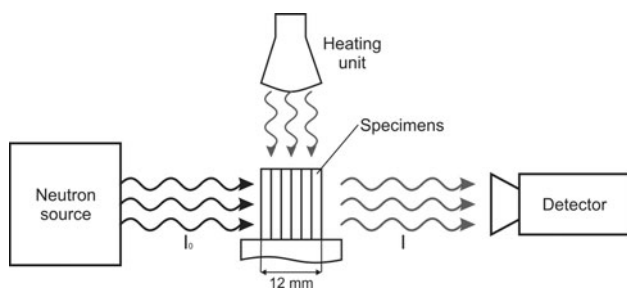
As seen in Fig. 1, hydrogen is only released at the extraction temperature of approximately 400 °C. This means that hydrogen is only located at interstitial sites in the lattice. Because technical iron is almost free of precipitations, carbides and inclusions, no hydrogen is bonded at so-called trapping sites. At 650 °C and 900 °C, hydrogen would be released from these different kinds of traps, but no such peaks are visible. Integration of the signal in Fig. 1 over time yields the total amount of hydrogen dissolved in the sample. A suitable calibration of the signal allows for calculation of the corresponding hydrogen concentration.

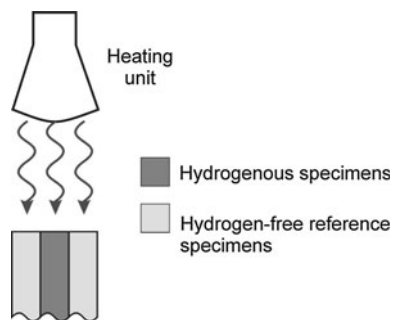### In situ analysis of hydrogen concentration

Experiments were performed at the ANTARES neutron imaging facility at the FRM II research reactor, Technische Universität München. The employed experimental setup is shown schematically in Fig. 2.
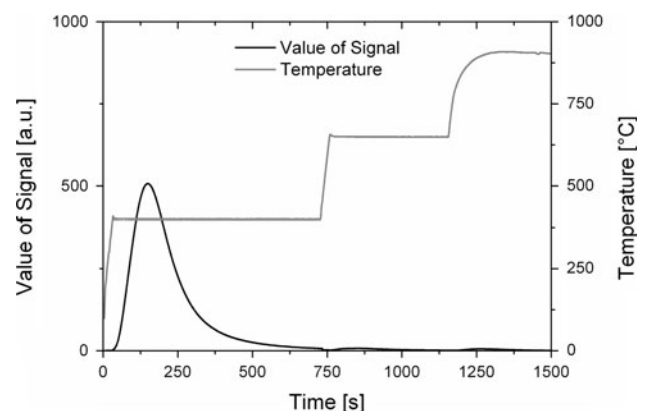
Fig. 1 Carrier gas hot extraction signal of hydrogenated technical iron as a function of time and temperature

Table 1 Measured chemical composition of austenitic stainless steel 1.4301 (wt%)

Fe	C	Ni	N	Mn	Cr	Mo	S
>99.7	0.002	0.013	0.0022	0.05	0.013	0.002	0.0033

Fig. 2 Schematic of the neutron radiography experimental setup

Fig. 3 Schematic of the sample arrangement in the direction of the neutron source

Fig. 4 Neutron radiography image of hydrogenous and hydrogen-free samples; the *rectangle* denotes a typical sample area used for measuring the average intensity of the transmitted beam

Radiography was performed with a neutron-sensitive scintillation screen, consisting of Cu- and Ag-doped 6LiF-ZnS, and a Peltier-cooled charge-coupled device (CCD) detector (Typ Andor DW436 N-BV) that viewed the screen via a mirror. With neutron flux of 1.0×10^8 n/cm^2 for $L/D = 400$ (where L is the pinhole–sample distance and D is the pinhole size) and average effective pixel size of 70 μm, the exposure time for an image was 28 s, including camera readout time, and images were recorded every 5 min. An infrared heat source allowed desorption experiments to be performed at higher temperatures. In each experiment, six hydrogenous samples, which were aligned to form a stack, were analysed. The stack had a thickness of $d = 12$ mm, showing maximum contrast between the hydrogen-loaded samples in the middle and the hydrogen-free sample at both sides (Fig. 3).

All samples were fixed in a sample holder covering the lower 10 mm. Three type K thermocouples with diameter of 0.5 mm were installed at 10 mm intervals, starting at the top of the sample, to measure the temperature during the course of the experiments. Figure 4 shows a neutron radiography image.

Using ImageJ software, the raw image was processed by subtracting the dark image and then dividing by the open beam image, from which the dark image was also subtracted, in order to minimise background noise and correct for image artefacts. The intensity was determined for a total surface area of 30 mm × 4.5 mm for each sample stack. The total area needed to be reduced due to the coverage of the lower 10 mm by the sample holder and a minimal shift of some samples in the stack. For the stacks of hydrogen-free samples, the mean value was calculated.

Results and discussion

Hydrogen concentration as a function of temperature and time was examined ex post in parallel experiments using carrier gas hot extraction. The temperature–time profile was the same as that used in the neutron radiography experiments and is shown in Fig. 5. The samples were first heated at a heating rate of 10 K/min, and after 20 min the heating rate was reduced to 4 K/min to slow down hydrogen desorption. The initial hydrogen concentration at
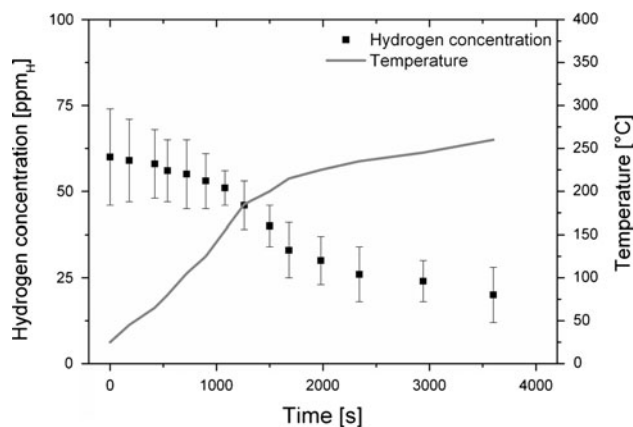
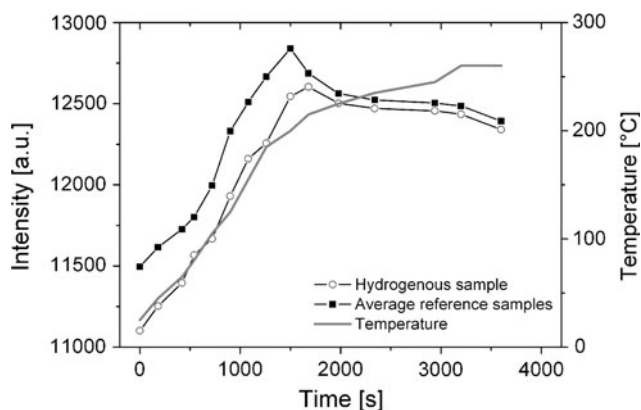**Fig. 5** Hydrogen concentration as a function of time and temperature

room temperature was 60 ppm$_H$. In combination with the results obtained from the neutron radiography experiment, the desorption behaviour as a function of time and temperature was determined and is also shown in Fig. 5.

Besides, a specific hydrogen concentration was assigned to every mean intensity value of the NR transmission images. With increasing temperature up to 200 °C, the hydrogen concentration decreased. With reduced heating for $t > 1,500$ s, the decrease of the hydrogen concentration in the samples slows down. The standard deviation is 8 ppm$_H$ on average. So, hydrogen quantification for concentrations lower than 30 ppm$_H$ is possible, although to minimise the error, reliable calibration standards need to be developed. Hydrogen concentrations lower than 20 ppm$_H$ are currently not detectable, because in this range hydrogen cannot be distinguished from background noise.

In the future, titanium hydride powder (TiH$_2$) will be used as a reference standard for determining hydrogen concentrations. A SiC/TiH$_2$ powder mixture can store hydrogen till temperatures of approximately 300 °C. Various powder mixtures will be measured to obtain a calibration function that will enable specific hydrogen concentrations that can be assigned to their corresponding intensity.

Analysis of the obtained neutron radiography images allows the determination of the intensity of the samples as a function of time and temperature (Fig. 6). To compare the hydrogenous samples with the hydrogen-free samples, the average was calculated for the stacks of hydrogen-free specimen.

The results of the hydrogenous and hydrogen-free samples were compared to establish the desorption behaviour. As shown in Fig. 6, the initial intensity for the hydrogenous samples was 11,100, in comparison with an initial intensity of 11,500 for the hydrogen-free samples. So, a hydrogen concentration of HD = 60 ppm$_H$ corresponds to an intensity difference of 400. As the temperature

increases, the desorption process starts and the intensity also increases, due to the lower amount of hydrogen in the samples to attenuate the neutrons. After heating for 1,500 s and an increase of temperature up to 200 °C, the intensity for the hydrogenous samples increased to 12,500 whereas that for the hydrogen-free samples increased to 12,850. So, a hydrogen concentration of HD = 25 ppm$_H$ corresponds to an intensity difference of 350. This means that, in comparison with the results from the carrier gas hot extraction, 60% of the diffusible hydrogen has now been released, due to the low activation energy of the diffusible hydrogen. If heating continues again for 35 min and the temperature reaches a maximum of 260 °C at the top of the samples, most of the hydrogen is desorbed, because the final intensities are nearly at the same level. The difference between the hydrogen-free reference samples and the hydrogenous samples is 50, which corresponds to a hydrogen concentration of HD = 20 ppm$_H$.

In Fig. 7, transmission is shown as a function of temperature and time. The transmission is the ratio between the intensity of the hydrogenous samples and the intensity of the hydrogen-free samples. This enables evaluation of the desorption behaviour as well as the possible lattice distortion effect of hydrogen.

As seen in Fig. 7, it can be stated that, with increasing temperature, hydrogen desorbs, leading to an increase of the transmission ratio. In fact, at room temperature the transmission ratio is 0.965. With the increase of temperature up to 200 °C, the transmission ratio increases to 0.977, then the transmission ratio increases strongly to 0.993, which correlates directly with faster desorption of hydrogen from the sample. Finally, the transmission nearly reaches a steady state at a transmission ratio of 0.995. If the transmission ratio were to reach unity, the hydrogen in the hydrogenous samples would have been fully desorbed.

Fig. 6 Intensity of the hydrogenous and the hydrogen-free samples as a function of time and temperature
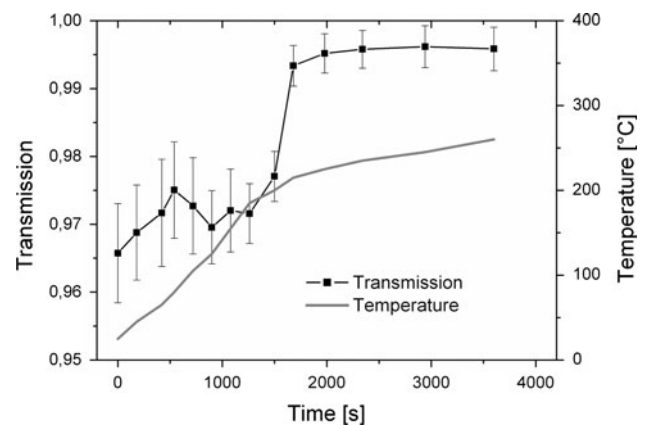
Fig. 7 Calculated transmission ratio between the intensity of the hydrogenous samples and that of the hydrogen-free samples as a function of temperature and time

It can be stated that the hydrogen desorption behaviour is strongly dependent on the temperature and that different amounts of desorbed hydrogen can be detected using neutron radiography. In comparison with Lehmann [23] or Sakaguchi [24, 25] it was possible to detect hydrogen amounts lower than 100 ppm$_H$, because the final detected hydrogen concentration was 20 ppm$_H$. In general, this would correspond to a reduction of the detection limit by 80%, although a direct comparison is not possible due to the use of a different facility, beam and detector arrangement.

Conclusions and outlook

Neutron radiography is a suitable technique to study the hydrogen desorption behaviour of technical iron. Separate carrier gas hot extraction experiments using the same temperature–time profile as for the neutron radiography experiment were used to calibrate the grey values of the neutron radiography images into hydrogen concentrations. The current detection limit for hydrogen in steel is 20 ppm$_H$ and may be reduced by modifying the measurement method through the introduction of reference standards of known concentrations. It can be stated that hydrogen desorption correlates with specimen temperature.

A future aim of such neutron radiography experiments is in situ determination of concentration-dependent diffusion coefficients. In desorption experiments at constant temperature, the diffusion coefficient D can be determined by evaluating the change of the hydrogen concentration C as a function of time t using an appropriate solution of Fick's second diffusion equation [27]. Furthermore, lattice distortion due to hydrogen uptake will be investigated using Bragg-edge neutron radiography.

References

1. Nelson HG (1983) In: Briant CL, Banerji SK (eds) Treatise on materials science and technology, vol 25. Academic, New York, p 275
2. Berkowitz J (1975) Hydrogen induced internal cracking of iron. State University of New York, Stony Brook, New York
3. Birnbaum HK (1995) Hydrogen related second phase embrittlement of solids. In: Gibala R, Hehemann RF (eds) Hydrogen embrittlement and stress corrosion cracking. ASM Int, Materials Park, p 153
4. Troiano AR (1960) Trans ASM 52:54
5. Stroe ME (2006) Hydrogen embrittlement of ferrous materials. Université Libre de Bruxelles, Brussels. http://theses.ulb.ac.be/ETD-db/collection/available/ULBetd-03312006-122217/unrestricted/HydrogenEmbrittlementofFerrousMaterials.pdf. Accessed 08 Feb 2011
6. Zapffe CA, Sims CE (1941) Trans AIME 145:225
7. Oriani RA (1987) Corrosion 43:390
8. Oriani RA (1995) In: Gibala R, Hehemann RF (eds) Hydrogen embrittlement and stress corrosion cracking. ASM Int, Materials Park, pp 43–59
9. Birnbaum HK, Sofronis P (1994) Mat Sci Eng A 176:191
10. Petch NJ, Stables P (1952) Nature 169:842
11. Geberich WW, Stauffer DD, Sofronis P (2008) In: Somerday B, Sofronis P, Jones R (eds) Effects of hydrogen on materials, 1st edn. ASM Int, Materials Park
12. Dadfarnia M, Novak P, Ahn DC, Liu JB, Sofronis P, Johnson DD, Robertson IM (2010) Adv Mater 22:1128
13. Olden V, Thaulow C, Johnson R (2008) Mater Des 29:1934
14. Hirth JP (1980) Metall Trans 11A:861
15. Quick NR, Johnson HH (1979) Metall Trans 10A:67
16. Ried P, Gaber M, Beyer K, Müller R, Kipphardt H, Kannengiesser T (2011) Steel Res Int 82:14
17. Robertson IM, Birnbaum HK (1986) Acta Metall Mater 34:353
18. Barnoush A, Bies C, Vehoff H (2008) J Mater Res 24:1105
19. Barnoush A, Zamanzade M, Vehoff H (2010) Scr Mater 62:242
20. Bergers K, Camisão de Souza E, Thomas I, Mabho N, Flock J (2010) Steel Res Int 81:499
21. Dabah E, Lisitsyn V, Eliezer D (2010) Mater Sci Eng A 527:4851
22. Balaskó M, Sva E, Kuba A, Kiss Z, Rodek L, Nagy A (2005) Nucl Instrum Methods A 542:302
23. Lehmann EH, Vontobel P, Kardjilov N (2004) Appl Radiat Isot 61:503
24. Sakaguchi H, Kohzai A, Hatakeyama K, Fujine S, Yoneda K, Kanda K, Esaka T (2000) Int J Hydrog Energy 25:1205
25. Sakaguchi H, Satake Y, Hatakeyama K, Fujine S, Yoneda K, Matsubayashi M, Esaka T (2003) J Alloy Compd 54:208
26. Schröder A, Wippermann K, Mergel J, Lehnert W, Stolten D, Sanders T, Baumhöfer T, Sauer DU, Manke I, Kardjilov N, Hilger A, Schloes J, Bahnhart J, Hartnig C (2009) Electrochem Commun 11:1606
27. Crank J (1975) The mathematics of diffusion. Clarendon, Oxford